UDC 621.3.013 https://doi.org/10.20998/2074-272X.2025.1.07

B.I. Kuznetsov, T.B. Nikitina, I.V. Bovdui, K.V. Chunikhin, V.V. Kolomiets, B.B. Kobylianskyi

Multispheroidal model of magnetic field of uncertain extended energy-saturated technical object

Problem. *The implementation of strict requirements for magnetic silence of elongated energy-saturated technical objects – such as naval vessel and submarines is largely determined by the adequacy of mathematical models to the signatures of a real magnetic field.* ***Aim***. *Simplification of mathematical modeling of the magnetic field of an uncertain extended energy-saturated object based on the development and application of a multispheroidal model of its magnetic field instead of the well-known multidipole model.* ***Methodology.*** *Coordinates of the geometric location and magnitudes of spatial extended spheroidal harmonics of spheroidal sources of multispheroidal model of magnetic field calculated as magnetostatics geometric inverse problems solution in the form of nonlinear minimax optimization problem based on near field measurements for prediction far extended technical objects magnetic field magnitude. Nonlinear objective function calculated as the weighted sum of squared residuals between the measured and predicted magnetic field COMSOL Multiphysics software package used. Nonlinear minimax optimization problems solutions calculated based on particle swarm nonlinear optimization algorithms.* ***Results.*** *Results of prediction far magnetic field magnitude of extended technical objects based on designed multispheroidal model of the magnetic field in the form of spatial prolate spheroidal harmonics in prolate spheroidal coordinate system using near field measurements with consideration of extended technical objects magnetic characteristics uncertainty.* ***Originality.*** *For the first time the method for design of multispheroidal model of magnetic field of uncertain extended energy-saturated technical object based on magnetostatics geometric inverse problems solution and magnetic field spatial spheroidal harmonics calculated in prolate spheroidal coordinate system taking into account of technical objects magnetic characteristics uncertainties developed.* ***Practical value.*** *It is shown the possibility to reduce the number of spheroidal sources of the magnetic field for adequate modeling of the real magnetic field based on the developed multispheroidal model compared to the number of well-known dipole sources of the magnetic field in the multidipole model of the magnetic field.* References 48, figures 4.

Key words: **energy-saturated extended technical objects, magnetic field, multispheroidal model, magnetic silencing, extended spheroidal coordinate system, spatial extended spheroidal harmonics.**

Проблема. *Реалізація жорстких вимог щодо «магнітної тиші» витягнутих енергонасичених технічних об'єктів – таких як військові кораблі та підводні човни, значною мірою визначається адекватністю математичних моделей сигнатурам реального магнітного поля цих об'єктів.* ***Мета.*** *Спрощення математичного моделювання магнітного поля невизначеного видовженого енергонасиченого об'єкта на основі розробки та застосування мультисфероїдальної моделі його магнітного поля замість відомої мультидипольної моделі.* ***Методологія.*** *Координати геометричного розташування та величини просторових витягнутих сфероїдних гармонік сфероідальних джерел мультисфероїдальної моделі магнітного поля витягнутих технічних об'єктів розраховані як розв'язок обернених геометричних задач магнітостатики в формі нелінійної задачі мінімаксної оптимізації на основі вимірювань ближнього поля для прогнозування величини магнітного поля витягнутих технічних об'єктів. Нелінійна цільова функція розрахована як зважена сума квадратів залишків між виміряним і прогнозованим магнітним полем з використанням програмного пакету COMSOL Multiphysics. Розв'язки задач нелінійної мінімаксної оптимізації розраховані на основі алгоритмів нелінійної оптимізації рою частинок.* ***Результати.*** *Результати прогнозування величини віддаленого магнітного поля витягнутих технічних об'єктів на основі спроектованої мультисфероїдальної моделі магнітного поля в вигляді просторових витягнутих сфероїдальних гармонік в витягнутій сфероїдній системі координат з використанням вимірювань ближнього поля та з врахуванням невизначеності магнітних характеристик витягнутих технічних об'єктів.* ***Оригінальність***. *Вперше розроблено метод проектування мультисфероїдальної моделі магнітного поля невизначеного витягнутого енергонасиченого технічного об'єкта на основі розв'язку геометричних обернених задач магнітостатики та обчислення просторових сфероїдальних гармонік магнітного поля в витягнутій сфероїальній системі координат з врахуванням невизначеності магнітних характеристик технічного об'єкта.* ***Практична цінність***. *Показана можливість зниження кількості сфероідальних джерел магнітного поля для адекватного моделювання реального магнітного поля на основі розробленої мультісфероїдальної моделі в порівнянні із кількістю дипольних джерел магнітного поля в відомій мультідипольній моделі магнітного поля.* Бібл. 48, рис. 4.

Ключові слова: **енергонасичені витягнуті технічні об'єкти, магнітне поле, мультисфероїдальна модель, магнітна тиша, витягнута сфероїдна система координат, просторові витягнуті сфероїдні гармоніки**.

Introduction. Most mathematical models of the magnetic field of energy-saturated technical objects are designed on the basis of multi-dipole models. Such models are widely used to simulate the magnetic field of spacecraft, naval vessel, submarines and other energy-saturated technical objects [1–9]. The number of dipoles in the mathematical model of the magnetic field is determined by the required accuracy of modeling the magnetic field of a real technical object can be 20 dipoles, 39 dipoles, or more dipoles [10–13].

For spacecraft, in addition to the magnitude of the magnetic field at the installation point of the on-board magnetometer, an important technical characteristic is also the magnitude of the magnetic moment of the spacecraft. Therefore, at the stage of design, production of elements and testing of spacecraft, the magnitude of the magnetic moment is compensated, so that the magnitude of the resulting magnetic moment of the spacecraft becomes very small. In this case, the main share of the spacecraft's magnetic field is generated not by dipoles, but by quadrupole, octupole and higher harmonics, and the model of the spacecraft's magnetic field is taken in the form of a multipole model [14].

For extended energy-saturated technical objects, the mathematical model of the magnetic field is most simply considered not in a spherical or rectangular coordinate system, but in an elongated spheroidal coordinate system. Naturally, for such objects it is most appropriate to consider the mathematical model of the magnetic field not in the form of a multidipole model, but in the form of a multispheroidal model of the magnetic field [15–18].

Due to the fact that the characteristics of the magnetic field of a technical object are known inaccurately and change during operation, when designing a mathematical model of the magnetic field, it is necessary to take into account the uncertainties of the magnetic characteristics of the technical object [4].

The goal of the work is simplification of mathematical modeling of the magnetic field of an uncertain extended energy-saturated object based on the development and application of a multispheroidal model of its magnetic field instead of the well-known multidipole model.

Problem statement. The external magnetic field of an elongated energy-saturated technical object is generated by engines, electric generators, electric motors, distribution boards and many other consumers of electrical energy [19–21]. Let's consider the design of a multispheroidal mathematical model that adequately describes the real magnetic field of an elongated energy-saturated technical object in an elongated spheroidal coordinate system associated with the center of the technical object.

In contrast to the multi-dipole model, which is widely used to model the external magnetic field of elongated energy-saturated technical objects [1–13], we assume that at the *i* points of an elongated energy-saturated technical object with coordinates (x_i, y_i, z_i) in the orthogonal system coordinates associated with the center of the technical object are located *I* sources of not a dipole, but a spheroidal magnetic field sources [22, 23]. These *I* sources generate a magnetic field at *J* measurement points with coordinates (x_j, y_j, z_j) in rectangular coordinate systems associated with the center of the technical object.

The layout of spheroidal magnetic field sources at points with the coordinates (x_i, y_i, z_i) and measuring points with the coordinates(x_j, y_j, z_j) in rectangular coordinate systems associated with the center of the extended energy-saturated technical object shown in Fig. 1.

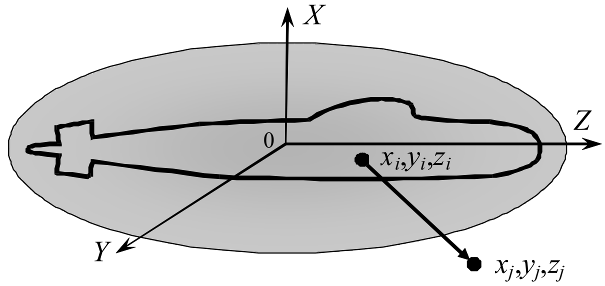

Fig. 1. The extended energy-saturated technical object

Then the components $H_{\xi ij}$, $H_{\eta ij}$, $H_{\varphi ij}$ of the magnetic field generated by these *I* spheroidal sources at *J* measurement points are calculated at points with coordinates ξ_{ij}, η_{ij}, φ_{ij} in elongated spheroidal coordinate systems associated with the centers of these sources, according to the following dependencies [18]:

$$
\begin{aligned}
H_{\xi ij} &= -\frac{\sqrt{\xi_{ij}{}^2-1}}{c_i\sqrt{\xi_{ij}{}^2-\eta_{ij}^2}}\sum_{n=1}^{\infty}\sum_{m=0}^{n}\frac{\mathrm{d}Q_{ni}^m(\xi_{ij})}{\mathrm{d}\xi_{ij}}\left\{c_{ni}^m\cos(m\varphi_{ij})+s_{ni}^m\sin(m\varphi_{ij})\right\}P_{ni}^m\left(\cos(\eta_{ij})\right);\\
H_{\eta ij} &= -\frac{\sqrt{1-\eta_{ij}{}^2}}{c_i\sqrt{\xi_{ij}{}^2-\eta_{ij}{}^2}}\sum_{n=1}^{\infty}\sum_{m=0}^{n}Q_{ni}^m(\xi_{ij})\frac{\mathrm{d}P_{ni}^m\left(\cos(\eta_{ij})\right)}{\mathrm{d}\eta_{ij}}\left\{c_{ni}^m\cos(m\varphi_{ij})+s_{ni}^m\sin(m\varphi_{ij})\right\};\\
H_{\varphi ij} &= \frac{m}{c_i\sqrt{\left(\xi_{ij}{}^2-1\right)\left(1-\eta_{ij}{}^2\right)}}\sum_{n=1}^{\infty}\sum_{m=0}^{n}Q_{ni}^m(\xi)P_{ni}^m\left(\cos(\eta_{ij})\right)\left\{c_{ni}^m\sin(m\varphi_{ij})-s_{ni}^m\cos(m\varphi_{ij})\right\}.
\end{aligned}
\quad (1)
$$

Here are the spherical coordinates ξ_{ij}, η_{ij}, φ_{ij} of observation points of the space of a technical object with coordinates (x_j, y_j, z_j) in rectangular coordinate systems associated with the center of the technical object, from the location points of spheroidal magnetic field sources with coordinates (x_i, y_i, z_i) in an orthogonal system coordinates associated with the center of the technical object are related by the relation

$$
\left.
\begin{aligned}
x_j-x_i &= c_i\cdot\sqrt{\xi_{ij}{}^2-1}\cdot\sqrt{1-\eta_{ij}{}^2}\cos\left(\varphi_{\mathrm{ij}}\right);\\
y_j-y_i &= c_i\cdot\sqrt{\xi_{ij}{}^2-1}\cdot\sqrt{1-\eta_{ij}{}^2}\sin\left(\varphi_{\mathrm{ij}}\right);\\
z_j-z_i &= c_i\cdot\xi_{ij}\cdot\eta_{ij};
\end{aligned}
\right\}
\Rightarrow
\begin{aligned}
\xi_{ij} &\in[1,\infty[;\\
\eta_{ij} &\in[0,1];\\
\varphi_{ij} &\in[0,2\pi];
\end{aligned}
\quad (2)
$$

where $P_{ni}^m\left(\xi_{ij}\right)$, $Q_{ni}^m\left(\xi_{ij}\right)$ associated Legendre functions of the first and second kind, respectively, with degree *n* and order *m*; c_i, c_{ni}^m, s_{ni}^m – constant coefficients characterizing the amplitudes of external spheroidal harmonics of the magnetic field.

Practical measurements and calculations of magnetic field components it is more convenient to carry out in the orthogonal coordinate system (x_j, y_j, z_j), the transition to which for the components H_{xij}, H_{yij}, H_{zij} is carried out using the formulas [18]:

$$
\begin{aligned}
H_{xij} &= \xi_{ij}\cdot\frac{\sqrt{1-\eta_{ij}{}^2}}{\sqrt{\xi_{ij}{}^2-\eta_{ij}{}^2}}\cdot\cos\left(\varphi_{ij}\right)\cdot H_{\xi ij}-\eta_{ij}\cdot\frac{\sqrt{\xi_{ij}{}^2-1}}{\sqrt{\xi_{ij}{}^2-\eta_{ij}{}^2}}\cdot\cos(\varphi_{ij})\cdot H_{\eta ij}-\sin(\varphi_{ij})\cdot H_{\varphi ij};\\
H_{yij} &= \xi_{ij}\cdot\frac{\sqrt{1-\eta_{ij}{}^2}}{\sqrt{\xi_{ij}{}^2-\eta_{ij}{}^2}}\cdot\sin\left(\varphi_{ij}\right)\cdot H_{\xi ij}-\eta_{ij}\cdot\frac{\sqrt{\xi_{ij}{}^2-1}}{\sqrt{\xi_{ij}{}^2-\eta_{ij}^2}}\cdot\sin(\varphi_{ij})\cdot H_{\eta ij}+\cos(\varphi_{ij})\cdot H_{\varphi ij};
\end{aligned}
\quad (3)
$$

$$H_{zij}=\eta_{ij}\cdot\frac{\sqrt{\xi_{ij}^{2}-1}}{\sqrt{\xi_{ij}^{2}-\eta_{ij}^{2}}}\cdot H_{\xi ij}+\cdot\xi_{ij}\cdot\frac{\sqrt{1-\eta_{ij}^{2}}}{\sqrt{\xi_{ij}^{2}-\eta_{ij}^{2}}}\cdot H_{\eta ij}.$$

Practical harmonic analysis in elongated spheroidal coordinate system based on (1) or (3) requires the calculation of associated Legendre polynomials of the first $P_{ni}^{m}(\xi_{ij})$ and second $Q_{ni}^{m}(\xi_{ij})$ kind. Polynomials $Q_{ni}^{m}(\xi_{ij})$ of the second kind calculated using the well-known formula with a limitation on the number of terms of the infinite series [18]

$$Q_{ni}^{m}(\xi_{ij})=\frac{(-1)^{m}\cdot(2)^{m-1}\cdot(\xi_{ij}^{2}-1)^{\frac{m}{2}}}{\xi_{ij}^{n+m+1}}\times\sum_{k=0}^{\infty}\frac{\Gamma_i\left(\frac{n}{2}+\frac{m}{2}+k+\frac{1}{2}\right)\cdot\Gamma_i\left(\frac{n}{2}+\frac{m}{2}+k+1\right)}{\Gamma_i(k+1)\cdot\Gamma_i\left(n+k+\frac{3}{2}\right)\cdot\xi_{ij}^{2k}}. \quad (4)$$

The region $\xi\in[\xi_0, 4]$ places strict demands on the accuracy of $Q_{ni}^{m}(\xi_{ij})$ function calculations. Algorithms for direct calculation $Q_{ni}^{m}(\xi_{ij})$ obtained in the form of finite sums [18]

$$Q_{ni}^{m}(\xi_{ij})=\frac{P_{ni}(\xi_{ij})}{2}\cdot\ln\left(\frac{\xi_{ij}+1}{\xi_{ij}-1}\right)-\sum_{k=1}^{n}\frac{1}{k}\cdot\sum_{\lambda=0}^{m}C_{mi}^{\lambda}\cdot P_{k-1}^{\lambda}(\xi_{ij})\cdot P_{n-k}^{m-\lambda}(\xi_{ij})++\frac{(1-\delta(m,0))}{2}\times\ldots$$

$$\ldots\times\sum_{q=0}^{m-1}C_{mi}^{q}\cdot P_{ni}^{q}(\xi_{ij})\cdot(m-q-1)!\cdot\frac{(\xi_{ij}-1)^{m-q}-(\xi_{ij}+1)^{m-q}}{(-1)^{m-q-1}(\xi_{ij}^{2}-1)^{\frac{m-q}{2}}};$$

$$Q_{ni}^{m}(\xi_{ij})=\frac{(\xi_{ij}^{2}-1)^{\frac{m}{2}}n!m!}{2^{n+1}}\sum_{k=0}^{m}\frac{(k+n)!\,\Omega(m-k,\xi_{ij})}{k!(m-k)!}\sum_{\lambda=k}^{n}\frac{(\xi_{ij}-1)^{n-\lambda}(\xi_{ij}+1)^{\lambda-k}}{\lambda!(n+k-\lambda)!(\lambda-k)!(n-\lambda)!}-\ldots \quad (5)$$

$$\ldots-\sum_{k=1}^{n}\frac{1}{k}\sum_{\lambda=0}^{m}C_{mi}^{\lambda}P_{k-1}^{\lambda}(\xi_{ij})P_{n-k,i}^{m-\lambda}(\xi_{ij}),$$

where

$$\Omega(\nu,\xi_{ij})=\left\{\begin{array}{l}\nu=0\quad\ln\left(\frac{\xi_{ij}+1}{\xi_{ij}-1}\right)\\ \nu\neq0\quad(-1)^{\nu-1}(\nu-1)!\frac{(\xi_{ij}-1)^{\nu}-(\xi_{ij}+1)^{\nu}}{(\xi_{ij}^{2}-1)^{\nu}}\end{array}\right\}\qquad C_{n}^{k}=\frac{n!}{(n-k)!k!}.$$

Note that the calculation of the components $H_{\xi ij}$, $H_{\eta ij}$, $H_{\varphi ij}$ of the magnetic field in spheroidal coordinates ξ_{ij}, η_{ij}, φ_{ij} using (1) or components H_{xij}, H_{yij}, H_{zij} in the orthogonal coordinate system (x_j, y_j, z_j) using (3) generated by spheroidal sources of the magnetic field for given values of parameters c_i and spatial spheroidal harmonics c_{ni}^{m}, s_{ni}^{m} at measurement points with coordinates (x_j, y_j, z_j) is a direct problem of magnetostatics for spheroidal magnetic field sources [24–29].

Solution method. Let us introduce a vector $\boldsymbol{X}$ of the required parameters, the components of which are the coordinates (x_i, y_i, z_i) of the location I of the sources of the spheroidal magnetic field in the space of the technical object, as well as the values of the parameters c_i and spatial spheroidal harmonics c_{ni}^{m}, s_{ni}^{m} of these I spheroidal magnetic field sources [30–32].

Then, for a given vector $\boldsymbol{X}$ and for given vector $\boldsymbol{G}$ the components $H_{\xi ij}$, $H_{\eta ij}$, $H_{\varphi ij}$ of the magnetic field in spheroidal coordinates ξ_{ij}, η_{ij}, φ_{ij} calculated based on (1) and components H_{xij}, H_{yij}, H_{zij} in the orthogonal coordinate system (x_j, y_j, z_j) generated by these I spheroidal sources of magnetic field at measurement points with coordinates (x_j, y_j, z_j) calculated based on (3).

Then, based on this calculated components H_{xij}, H_{yij}, H_{zij} of the magnetic field generated by each element I the components H_{xj}, H_{yj}, H_{zj} of magnetic field generated by all I spheroidal sources of magnetic field at the measurement points J calculated in the orthogonal coordinate system (x_j, y_j, z_j) associated with the center of the technical object.

In this case, the axes of orthogonal coordinate systems of spheroidal magnetic field sources located in the space of a technical object with coordinates (x_i, y_i, z_i) are taken parallel to the orthogonal coordinate systems of magnetic field measurement points with coordinates (x_j, y_j, z_j) and parallel axes of orthogonal coordinate systems of the magnetic field of a technical object with zero coordinates.

With this choice of arrangement of axes of orthogonal coordinate systems, the values of the resulting magnetic field components H_{xj}, H_{yj}, H_{zj} at the measurement points are calculated in the form of sums of the corresponding magnetic field components H_{xij}, H_{yij}, H_{zij} generated by individual spheroidal magnetic field sources. Naturally, to calculate based on (3) the components H_{xij}, H_{yij}, H_{zij} in the orthogonal coordinate system (x_j, y_j, z_j) generated by these I spheroidal sources of magnetic field at measurement points with coordinates (x_j, y_j, z_j) the components $H_{\xi ij}$, $H_{\eta ij}$, $H_{\varphi ij}$ of the magnetic field in spheroidal coordinates ξ_{ij}, η_{ij}, φ_{ij} are first calculated based on (1).

A feature of energy-saturated extended technical objects is the uncertainty of the magnetic characteristics of their elements, as well as changes in their values in different operating modes [33–38]. Let us introduce the uncertainty vector $\boldsymbol{G}$ of parameters of energy-saturated extended technical object [41, 42].

Let us introduce a vector $\boldsymbol{Y_C}(\boldsymbol{X}, \boldsymbol{G})$ whose components are the components of the calculated values or components H_{xj}, H_{yj}, H_{zj} in the orthogonal coordinate system (x_j, y_j, z_j) of the magnetic field at J measurement points with coordinates (x_j, y_j, z_j).

Let us introduce a vector $\boldsymbol{Y_M}(\boldsymbol{G})$ whose components are the measured values H_{xj}, H_{yj}, H_{zj} in the orthogonal coordinate system (x_j, y_j, z_j) of the magnetic field at J measurement points with coordinates (x_j, y_j, z_j). Naturally, these measurements depend on the vector $\boldsymbol{G}$ of uncertainty parameters of the magnetic characteristics of the technical object.

Let us introduce the residual vector $\boldsymbol{E}(\boldsymbol{X}, \boldsymbol{G})$ of the vector $\boldsymbol{Y_M}(\boldsymbol{G})$ of the measured magnetic field and the vector $\boldsymbol{Y_C}(\boldsymbol{X}, \boldsymbol{G})$ of the magnetic field calculated according to multispheroidal model (3)

$$\boldsymbol{E(X,G)} = \boldsymbol{Y_M (G)} - \boldsymbol{Y_C (X,G)}\,. \qquad (6)$$

The nonlinear vector objective function (6) obtained based on (3) relative to the vector $\boldsymbol{X}$ of unknown required parameters, the components of which are the coordinates (x_i, y_i, z_i) of the location I of the sources of the spheroidal magnetic field in the space of the technical object, as well as the values of the parameters c_i and spatial spheroidal harmonics c_{ni}^{m}, s_{ni}^{m} of these I spheroidal magnetic field sources and uncertainty vector $\boldsymbol{G}$ of the parameters of the magnetic characteristics of a technical object.

This approach is standard when constructing a robust multispheroidal mathematical model of the magnetic field of an elongated, energy-saturated technical object, when the coordinates of the spatial location and the magnitude of spatial spheroidal harmonics are found from the conditions of minimizing the divergence vector between the vector of the measured magnetic field and the vector of the predicted one model of a magnetic field, but for the «worst» vector of parameters, the uncertainties of the magnetic characteristics of a technical object are found from the conditions of maximizing the same vector of the residual of the vector of the measured magnetic field and the vector of the magnetic field predicted by multispheroidal model.

Note that the calculation of the desired coordinates (x_i, y_i, z_i) of the spatial location I of spheroidal magnetic field sources, as well as the desired values of parameters c_i and spatial spheroidal harmonics c_{ni}^{m}, s_{ni}^{m} of these spheroidal magnetic field sources and the uncertainty vector $\boldsymbol{G}$ of the parameters of the magnetic characteristics of a technical object is geometric the inverse problem of magnetostatics for spheroidal magnetic field sources. Based on the obtained spheroidal model (3), it is possible to calculate and predict the magnitude of the magnetic field at any point in the far zone of a technical object and, therefore, prediction problem of the magnetic field of technical object solved.

In the course of solving this geometric inverse problem (6) of magnetostatics for a spheroidal magnetic field model, it is necessary to repeatedly solve the direct problem (3) when iteratively calculating the values of the desired coordinates desired coordinates (x_i, y_i, z_i) of the spatial location I of spheroidal magnetic field sources, as well as the desired values of parameters c_i and spatial spheroidal harmonics c_{ni}^{m}, s_{ni}^{m} of these spheroidal magnetic field sources and the uncertainty vector $\boldsymbol{G}$ of the parameters of the magnetic characteristics of a technical object.

The components of the vector game (6) are nonlinear functions of the vector $\boldsymbol{X}$ of required parameters and the vector $\boldsymbol{G}$ of uncertainty parameters of the geometric inverse problem of magnetostatics of predicting the magnetic field of a technical object, taking into account the uncertainties of the direct problem and calculated using COMSOL Multiphysical software.

When solving the geometric inverse problem of magnetostatics of predicting the magnetic field of technical objects, taking into account the uncertainties of the direct problem, a worst-case design approach is used to make the multi-spheroidal magnetic field model robust. In these cases, solving the inverse geometric forecasting problem comes down to solving a game in which the vector $\boldsymbol{X}$ of the required parameters – the first player minimizes the game payoff (6), but the vector $\boldsymbol{G}$ of uncertainties of the direct problem – the second player tries to maximize the same game payoff (6).

A feature of the considered problem of vector minimax optimization is the multi-extremal nature of the game payoff (6), so that the considered region of possible solutions contains local minima and maxima. Therefore, to calculate the solution to the vector game under consideration, stochastic multi-agent optimization algorithms are used [33–36].

The basic approach to multicriteria optimization is to find a Pareto set that includes all solutions that are not dominated by other solutions. To adapt the PSO method in relation to the problem of finding Pareto optimal solutions on the set of possible values of the vector criterion, binary preference relations are used that determine the Pareto dominance of individual solutions.

To calculate one global solution to the vector game (6), individual swarms exchange information with each other in the process of calculating optimal solutions to local games. Information about the global optimum obtained by particles from another swarm is used to calculate the speed of movement of particles from another swarm, which makes it possible to calculate all potential Pareto-optimal solutions [37–40]. To increase the speed of searching for a global solution, a nonlinear stochastic multi-agent optimization algorithm has recently been used, in which the movement of a swarm particle is described by the following expressions

$$\begin{aligned} v_{ij}(t+1) &= w_{1j}v_{ij}(t)+c_{1j}r_{1j}(t)H\big(p_{1ij}(t)-\varepsilon_{1ij}(t)\big)\big[y_{ij}(t)- \\ &- x_{ij}(t)\big]+c_{2j}r_{2j}(t)H\big(p_{2ij}(t)-\varepsilon_{2ij}(t)\big)\big[y_j^{*}(t)-x_{ij}(t)\big]; \end{aligned} \qquad (7)$$

$$\begin{aligned} u_{ij}(t+1) &= w_{2j}u_{ij}(t)+c_{3j}r_{3j}(t)H\big(p_{3ij}(t)-\varepsilon_{3ij}(t)\big)\big[z_{ij}(t)- \\ &- \delta_{ij}(t)\big]+c_{4j}r_{4j}(t)H\big(p_{4ij}(t)-\varepsilon_{4ij}(t)\big)\big[z_j^{*}(t)-\delta_{ij}(t)\big]; \end{aligned} \qquad (8)$$

$$x_{ij}(t+1) = x_{ij}(t)+v_{ij}(t+1); \quad g_{ij}(t+1) = \delta_{ij}(t)+u_{ij}(t+1)\,, \qquad (9)$$

where $x_{ij}(t)$, $g_{ij}(t)$ and $v_{ij}(t)$, $u_{ij}(t)$ is the position and velocity of i particle of j swarm. In (7) – (20) $y_{ij}(t)$, $z_{ij}(t)$ and $y_j^{*}(t)$, $z_j^{*}(t)$ – the best local and global positions of the i–th particle, found respectively by only one i-th particle and all the particles of j swarm. Moreover, the best local position $y_{ij}(t)$ and the global position $y_j^{*}(t)$ of the i particle of j swarm are understood in the sense of the first player strategy $x_{ij}(t)$ for minimum of component of the vector payoff (6). However, the best local position $z_{ij}(t)$ and the global position z_j^* of the i particle of j swarm are understood in the sense of the second player strategy $g_{ij}(t)$ for maximum of the same component of the vector payoff (6). Four independent random numbers $r_{1j}(t)$, $r_{2j}(t)$, $r_{3j}(t)$, $r_{4j}(t)$ are in the range of [0, 1], which determine the stochastic particle velocity components. Positive constants c_{1j}, c_{2j} and c_{3j}, c_{4j} determine the cognitive and social weights of the particle velocity components.

In random search, the motion of the particle is carried out in the direction of the maximum growth of the component of the objective function, found in the process of random search. In general, this direction serves as an estimate of the direction of the gradient in a random search. Naturally, such an increment of the objective function serves as an analogue of the first derivative – the rate of change of the objective function.

To take these constraints into account when searching for solutions special particle swarm optimization method for constrained optimization problems used [43]. To take these binary preference relations into account when searching for solutions special evolutionary algorithms for multiobjective optimizations used [44].

Simulation results. Let's consider the design of a mathematical model of an indefinite elongated energy-saturated object. A many number of studies have been devoted to measuring the actual signatures of the initial magnetic field of naval vessel and submarines [45–48]. Let us consider the initial data of the magnetic field of an energy-saturated elongated technical object [8]. The initial magnetic field generated by 16 dipoles located in the space of a technical object with coordinates $x = \pm 39$ m and ± 13 m with $y = \pm 4$ m and $z = 3.5$ m. These dipoles have different values of the magnetic moment components M_x, M_y and M_z along the three axes of the rectangular coordinate system. Magnetic field levels were calculated in the range from $x = -100$ m to $x = 100$ m for three values $y = 0$ and $y = \pm 20$ m. Thus, the three components of the magnetic field strength were calculated at 303 points, so that the total number of measurements was 909. In this case, the calculations were carried out for values $z = 19$ m.

Let us first consider the design of a mathematical model of a magnetic field in the form of one ellipsoid located in the center of a technical object, taking into account three harmonics. At the same time, in the course of solving the inverse problem of magnetostatics, the following values of the parameter $c = 45.2148$, and three harmonics were calculated

$c_1^0 = -2.975$, $c_1^1 = -0.784038$, $s_1^1 = -1.20929$,

$c_2^0 = -7.61817$, $c_2^1 = 1.02379$, $c_2^2 = -0.0247782$,

$s_2^1 = 0.321446$, $s_2^2 = 0.0175008$, $c_3^0 = 2.30691$,

$c_3^1 = -0.555912$, $c_3^2 = 0.00222368$, $c_3^3 = 0.000110636$,

$s_3^1 = 0.856451$, $s_3^2 = -0.0155754$, $s_3^3 = 0.000037359$.

In Fig. 2 shown signatures of projections of inductions of the original magnetic field of a technical object (solid lines) and models (dashed lines) for three coordinate values: *a*) $Y = -20$ m, $Z = 19$ m, *b*) $Y = 0$ m, $Z = 19$ m, *c*) $Y = 20$ m, $Z = 19$ m, d) induction modules of the original and model magnetic field of the technical object.

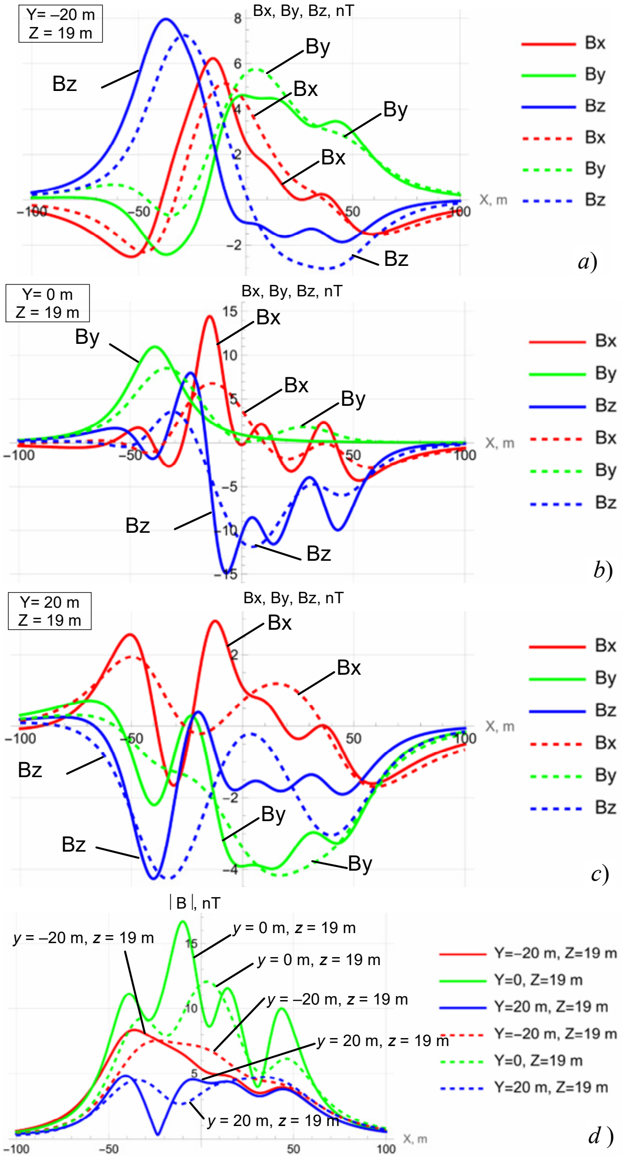

Fig. 2. Signatures of the original magnetic field and the model in the form of a single spheroid

Let us now consider the design of a mathematical model of a magnetic field in the form of three ellipsoids located in the space of a technical object, taking into account only the first spatial harmonics of these ellipsoids.

As a result of solving the geometric inverse problem of magnetostatics, the coordinates of the spatial location and values of the parameters c and first harmonics c_1^0, c_1^1, s_1^1 of these three ellipsoids calculated. Source $M_1 - x = -38.2288$ m, $y = 0.23875$ m, $z = -0.898403$ m, $c = 0.255598$, $c_1^0 = 2150.98$, $c_1^1 = -20787.9$, $s_1^1 = -5998.98$. Source $M_2 - x = -15.1439$ m, $y = 0.851608$ m, $z = 3.27869$ m, $c = 0.288814$, $c_1^0 = -17081.5$, $c_1^1 = 510.902$, $s_1^1 = 107.937$. Source $M_3 - x = 5.13809$ m, $y = 0.455979$ m, $z = -0.342088$ m, $c = 58.0619$, $c_1^0 = -1.63027$, $c_1^1 = 0.0270398$, $s_1^1 = -0.356172$.

In Fig. 3 shown signatures of projections of inductions of the original magnetic field of a technical object (solid lines) and models (dashed lines) for three coordinate values: *a*) $Y = -20$ m, $Z = 19$ m, *b*) $Y = 0$ m, $Z = 19$ m, *c*) $Y = 20$ m, $Z = 19$ m, *d*) induction modules of the original and model magnetic field of the technical object.

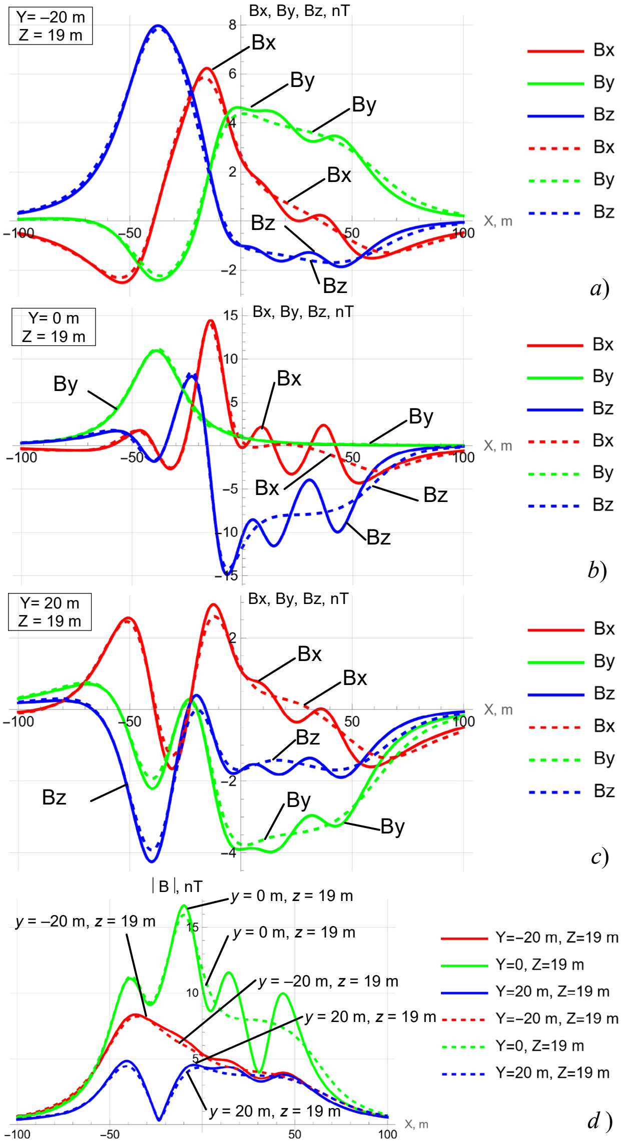

Fig. 3. Signatures of the initial magnetic field and the multispheroidal model in three ellipsoids form

Thus, the multispheroidal model of the magnetic field of an elongated technical object in the form of three spheroids, in which only the first spatial harmonics were taken into account. Describes the initial magnetic field significantly more adequately compared to the single-sphere model, even when taking into account three harmonics, as shown in Fig. 3.

Let us now consider the design of a mathematical model of a magnetic field in the form of four ellipsoids located in the space of a technical object, taking into account only the first spatial harmonics of these ellipsoids. As a result of solving the geometric inverse problem of magnetostatics, the coordinates of the spatial location and values of the parameters c and first harmonics c_1^0, c_1^1, s_1^1 of these four ellipsoids calculated.

1) Source M_1 – x = 24.1775 m, y = 0.203945 m, z = 1.44653 m, c = 17.1245, c_1^0 = –840.073, c_1^1 = 13.9223, s_1^1 = –193.016.

2) Source M_2 – x = –13.2818 m, y = 0.498642 m, z = 0.266331 m, c = 0.232014, c_1^0 = –58875.5, c_1^1 = 1373.1, s_1^1 = –7953.4.

3) Source M_3 – x = –38.496 m, y = 0.276427 m, z = –1.03295 m, c = 0.337585, c_1^0 = –3620.08, c_1^1 = –11852.2, s_1^1 = –3933.69.

4) Source M_4 – x = 24.1911 m, y = 0.203772 m, z = 1.4617 m, c = 16.9606, c_1^0 = 847.093, c_1^1 = –14.0885, s_1^1 = 194.566.

In Fig. 4 shown signatures of projections of inductions of the original magnetic field of a technical object (solid lines) and models (dashed lines) for three coordinate values: *a*) Y = –20 m, Z = 19 m, *b*) Y = 0 m, Z = 19 m, *c*) Y = 20 m, Z = 19 m, *d*) induction modules of the original and model magnetic field of the technical object.

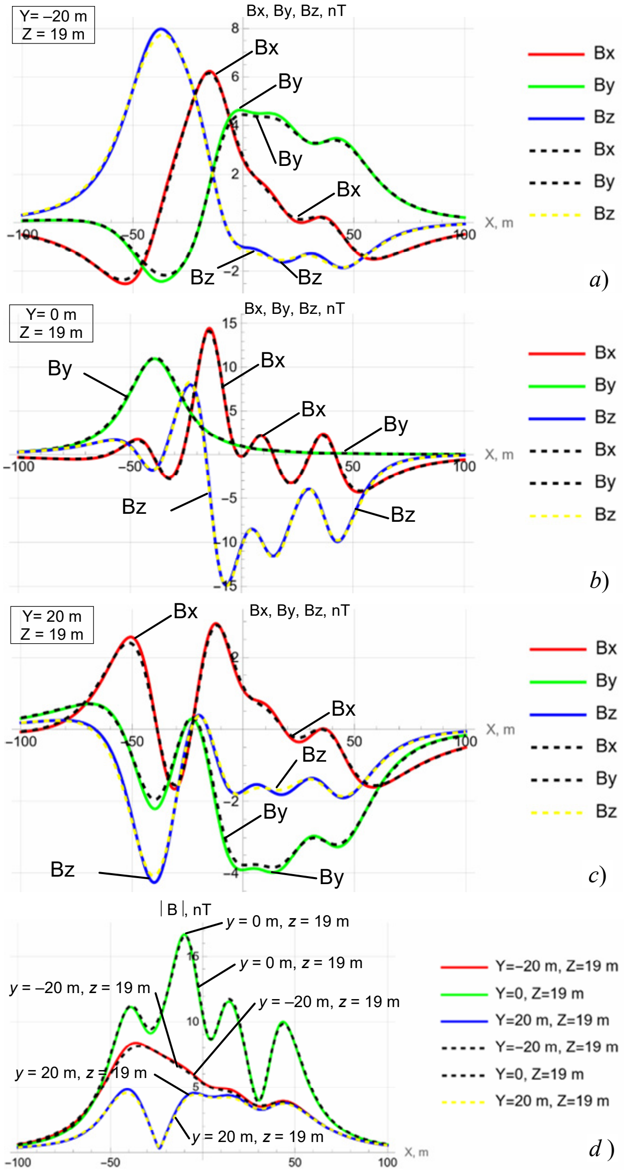

Fig. 4. Signatures of the initial magnetic field and the multispheroidal model in four ellipsoids form

Thus, the multispheroidal model of the magnetic field of an elongated technical object in the form of four spheroids, in which only the first spatial harmonics were taken into account, almost accurately describes the original magnetic field of the technical object, specified in the form of 16 magnetic dipoles located in the space of the technical object.

Conclusions.

1. For the first time the method for design of multispheroidal model of magnetic field of uncertain extended energy-saturated technical object for simplification of mathematical modeling of the magnetic field of an uncertain extended energy-saturated object instead of the well-known multidipole model. Design of multispheroidal model based on magnetostatics geometric inverse problems solution and magnetic field spatial spheroidal harmonics calculated in prolate spheroidal coordinate system taking into account of technical objects magnetic characteristics uncertainties developed.
2. Coordinates of the geometric location and magnitudes of spatial extended spheroidal harmonics of spheroidal sources of multispheroidal model of magnetic field calculated as magnetostatics geometric inverse problems solution in the form of nonlinear minimax optimization problem based on near field measurements for prediction far extended technical objects magnetic field magnitude. Nonlinear objective function calculated as the weighted sum of squared residuals between the measured and predicted magnetic field COMSOL Multiphysics software package used. Nonlinear minimax optimization problems solutions calculated based on particle swarm nonlinear optimization algorithms.
3. Based on the developed multispheroidal model, the signature of extended energy-saturated technical object simulated. The initial magnetic field generated by 16 dipoles located in the space of the object. Using the designed multispheroid model, the initial magnetic field in the form of 4 spheroidal magnetic field sources adequately approximated.
4. Based on the results of using the developed multispheroidal model, it is shown the possibility to reduce the number of spheroidal sources of the magnetic field for adequate modeling of the real magnetic field based on the developed multispheroidal model compared to the number of dipole sources of the magnetic field in the well-known multidipole model of the magnetic field more than 4 times.

Acknowledgments. The authors express their gratitude to the researcher Anatoliy Erisov of the department of magnetism of technical object of Anatolii Pidhornyi Institute of Mechanical Engineering Problems of the National Academy of Sciences of Ukraine for the kindly provided materials on the results of experimental measured magnetic field generated by energy-saturated technical objects and also for numerous discussions that allowed the authors to improve the article manuscript.

REFERENCES

1. Rozov V.Yu., Getman A.V., Petrov S.V., Erisov A.V., Melanchenko A.G., Khoroshilov V.S., Schmidt I.R Spacecraft magnetism. *Technical Electrodynamics. Thematic issue «Problems of modern electrical engineering»*, 2010, part 2, pp. 144-147. (Rus).

2. Rozov V.Yu. Methods for reducing external magnetic fields of energy-saturated objects. *Technical Electrodynamics*, 2001, no. 1, pp. 16-20.

3. Rozov V.Yu. Selective compensation of spatial harmonics of the magnetic field of energy-saturated objects. *Technical Electrodynamics*, 2002, no. 1, pp. 8-13. (Rus).

4. *ECSS-E-HB-20-07A. Space engineering: Electromagnetic compatibility hand-book. ESA-ESTEC. Requirements & Standards Division*. Noordwijk, Netherlands, 2012. 228 p.

5. Droughts S.A., Fedorov O.P. Space project Ionosat-Micro. Monograph. Kyiv, Akademperiodika Publ., 2013. 218 p. (Rus).

6. Holmes J.J. *Exploitation of A Ship's Magnetic Field Signatures*. Springer Cham, 2006. 67 p. doi: https://doi.org/10.1007/978-3-031-01693-6.

7. Woloszyn M., Jankowski P. Simulation of ship's deperming process using Opera 3D. *2017 18th International Symposium on Electromagnetic Fields in Mechatronics, Electrical and Electronic Engineering (ISEF) Book of Abstracts*, 2017, pp. 1-2. doi: https://doi.org/10.1109/ISEF.2017.8090680.

8. Birsan M., Holtham P., Carmen. Using global optimisation techniques to solve the inverse problem for the computation of the static magnetic signature of ships. *Defense Research Establishment Atlantic*, 9 Grove St., PO Box 1012, Dartmouth, Nova Scotia, B2Y 3Z7, Canada.

9. Zuo C., Ma M., Pan Y., Li M., Yan H., Wang J., Geng P., Ouyang J. Multi-objective optimization design method of naval vessels degaussing coils. *Proceedings of SPIE - The International Society for Optical Engineering*, 2022, vol. 12506, art. no. 125060J. doi: https://doi.org/10.1117/12.2662888.

10. Mehlem K., Wiegand A. Magnetostatic cleanliness of spacecraft. *2010 Asia-Pacific International Symposium on Electromagnetic Compatibility*, 2010, pp. 936-944. doi: https://doi.org/10.1109/APEMC.2010.5475692.

11. Messidoro P., Braghin M., Grande M. Magnetic cleanliness verification approach on tethered satellite. *16th Space Simulation Conference: Confirming Spaceworthiness into the Next Millennium*, 1991, pp. 415-434.

12. Mehlem K., Narvaez P. Magnetostatic cleanliness of the radioisotope thermoelectric generators (RTGs) of Cassini. *1999 IEEE International Symposium on Electromagnetic Compatability*, 1999, vol. 2, pp. 899-904. doi: https://doi.org/10.1109/ISEMC.1999.810175.

13. Eichhorn W.L. *Magnetic dipole moment determination by near-field analysis*. Goddard Space Flight Center. Washington, D.C., National Aeronautics and Space Administration, 1972. NASA technical note, D 6685. 87 p.

14. Rozov V.Yu., Dobrodeev P.N., Volokhov S.A. Multipole model of a technical object and its magnetic center. *Technical Electrodynamics*, 2008, no. 2, pp. 3-8. (Rus).

15. Rozov V.Yu., Getman A.V., Kildishev A.V. Spatial harmonic analysis of the external magnetic field of extended objects in a prolate spheroidal coordinate system. *Technical Electrodynamics*, 1999, no. 1, pp. 7-11. (Rus).

16. Rozov V.Yu. Mathematical model of electrical equipment as a source of external magnetic field. *Technical Electrodynamics*, 1995, no. 2, pp. 3-7. (Rus).

17. Volokhov S.A., Dobrodeev P.N., Ivleva L.F. Spatial harmonic analysis of the external magnetic field of a technical object. *Technical Electrodynamics*, 1996, no. 2, pp. 3-8. (Rus).

18. Getman A.V. *Analysis and synthesis of the magnetic field structure of technical objects on the basis of spatial harmonics*. Dissertation thesis for the degree of Doctor of Technical Sciences. Kharkiv, 2018. 43 p. (Ukr).

19. Xiao C., Xiao C., Li G. Modeling the ship degaussing coil's effect based on magnetization method. *Communications in Computer and Information Science*, 2012, vol. 289, pp. 62-69. doi: https://doi.org/10.1007/978-3-642-31968-6_8.

20. Wołoszyn M., Jankowski P. Ship's de-perming process using coils lying on seabed. *Metrology and Measurement Systems*, 2019, vol. 26, no. 3, pp. 569-579. doi: https://doi.org/10.24425/mms.2019.129582.

21. Fan J., Zhao W., Liu S., Zhu Z. Summary of ship comprehensive degaussing. *Journal of Physics: Conference Series*, 2021, vol. 1827, no. 1, art. no. 012014. doi: https://doi.org/10.1088/1742-6596/1827/1/012014.

22. Getman A.V. Spatial harmonic analysis of the magnetic field of the sensor of the neutral plasma component. *Eastern European Journal of Advanced Technologies*, 2010, vol. 6, no. 5(48), pp. 35-38. doi: https://doi.org/10.15587/1729-4061.2010.3326.

23. Getman A. Ensuring the Magnetic Compatibility of Electronic Components of Small Spacecraft. *2022 IEEE 3rd KhPI Week on Advanced Technology (KhPIWeek)*, 2022, no. 1-4. doi: https://doi.org/10.1109/KhPIWeek57572.2022.9916339.

24. Acuña M.H. *The design, construction and test of magnetically clean spacecraft – a practical guide*. NASA/GSFC internal report. 2004.

25. Junge A., Marliani F. Prediction of DC magnetic fields for magnetic cleanliness on spacecraft. *2011 IEEE International Symposium on Electromagnetic Compatibility*, 2011, pp. 834-839. doi: https://doi.org/10.1109/ISEMC.2011.6038424.

26. Lynn G.E., Hurt J.G., Harriger K.A. Magnetic control of satellite attitude. *IEEE Transactions on Communication and Electronics*, 1964, vol. 83, no. 74, pp. 570-575. doi: https://doi.org/10.1109/TCOME.1964.6539511.

27. Junge A., Trougnou L., Carrubba E. Measurement of Induced Equivalent Magnetic Dipole Moments for Spacecraft Units and Components. *Proceedings ESA Workshop Aerospace EMC 2009 ESA WPP-299*, 2009, vol. 4, no. 2, pp. 131-140.
28. Matsushima M., Tsunakawa H., Iijima Y., Nakazawa S., Matsuoka A., Ikegami S., Ishikawa T., Shibuya H., Shimizu H., Takahashi F. Magnetic Cleanliness Program Under Control of Electromagnetic Compatibility for the SELENE (Kaguya) Spacecraft. *Space Science Reviews*, 2010, vol. 154, no. 1-4, pp. 253-264. doi: https://doi.org/10.1007/s11214-010-9655-x.
29. Boghosian M., Narvaez P., Herman R. Magnetic testing, and modeling, simulation and analysis for space applications. *2013 IEEE International Symposium on Electromagnetic Compatibility*, 2013, pp. 265-270. doi: https://doi.org/10.1109/ISEMC.2013.6670421.
30. Mehlem K. Multiple magnetic dipole modeling and field prediction of satellites. *IEEE Transactions on Magnetics*, 1978, vol. 14, no. 5, pp. 1064-1071. doi: https://doi.org/10.1109/TMAG.1978.1059983.
31. Thomsen P.L., Hansen F. Danish Ørsted Mission In-Orbit Experiences and Status of The Danish Small Satellite Programme. *Annual AIAA/USU Conference on Small Satellites*, 1999, pp. SSC99-I–8.
32. Kapsalis N.C., Kakarakis S.-D.J., Capsalis C.N. Prediction of multiple magnetic dipole model parameters from near field measurements employing stochastic algorithms. *Progress In Electromagnetics Research Letters*, 2012, vol. 34, pp. 111-122. doi: https://doi.org/10.2528/PIERL12030905.
33. Solomentsev O., Zaliskyi M., Averyanova Y., Ostroumov I., Kuzmenko N., Sushchenko O., Kuznetsov B., Nikitina T., Tserne E., Pavlikov V., Zhyla S., Dergachov K., Havrylenko O., Popov A., Volosyuk V., Ruzhentsev N., Shmatko O. Method of Optimal Threshold Calculation in Case of Radio Equipment Maintenance. *Data Science and Security. Lecture Notes in Networks and Systems*, 2022, vol. 462, pp. 69-79. doi: https://doi.org/10.1007/978-981-19-2211-4_6.
34. Ruzhentsev N., Zhyla S., Pavlikov V., Volosyuk V., Tserne E., Popov A., Shmatko O., Ostroumov I., Kuzmenko N., Dergachov K., Sushchenko O., Averyanova Y., Zaliskyi M., Solomentsev O., Havrylenko O., Kuznetsov B., Nikitina T. Radio-Heat Contrasts of UAVs and Their Weather Variability at 12 GHz, 20 GHz, 34 GHz, and 94 GHz Frequencies. *ECTI Transactions on Electrical Engineering, Electronics, and Communications*, 2022, vol. 20, no. 2, pp. 163-173. doi: https://doi.org/10.37936/ecti-eec.2022202.246878.
35. Havrylenko O., Dergachov K., Pavlikov V., Zhyla S., Shmatko O., Ruzhentsev N., Popov A., Volosyuk V., Tserne E., Zaliskyi M., Solomentsev O., Ostroumov I., Sushchenko O., Averyanova Y., Kuzmenko N., Nikitina T., Kuznetsov B. Decision Support System Based on the ELECTRE Method. *Data Science and Security. Lecture Notes in Networks and Systems*, 2022, vol. 462, pp. 295-304. doi: https://doi.org/10.1007/978-981-19-2211-4_26.
36. Shmatko O., Volosyuk V., Zhyla S., Pavlikov V., Ruzhentsev N., Tserne E., Popov A., Ostroumov I., Kuzmenko N., Dergachov K., Sushchenko O., Averyanova Y., Zaliskyi M., Solomentsev O., Havrylenko O., Kuznetsov B., Nikitina T. Synthesis of the optimal algorithm and structure of contactless optical device for estimating the parameters of statistically uneven surfaces. *Radioelectronic and Computer Systems*, 2021, no. 4, pp. 199-213. doi: https://doi.org/10.32620/reks.2021.4.16.
37. Volosyuk V., Zhyla S., Pavlikov V., Ruzhentsev N., Tserne E., Popov A., Shmatko O., Dergachov K., Havrylenko O., Ostroumov I., Kuzmenko N., Sushchenko O., Averyanova Yu., Zaliskyi M., Solomentsev O., Kuznetsov B., Nikitina T. Optimal Method for Polarization Selection of Stationary Objects Against the Background of the Earth's Surface. *International Journal of Electronics and Telecommunications*, 2022, vol. 68, no. 1, pp. 83-89. doi: https://doi.org/10.24425/ijet.2022.139852.
38. Zhyla S., Volosyuk V., Pavlikov V., Ruzhentsev N., Tserne E., Popov A., Shmatko O., Havrylenko O., Kuzmenko N., Dergachov K., Averyanova Y., Sushchenko O., Zaliskyi M., Solomentsev O., Ostroumov I., Kuznetsov B., Nikitina T. Practical imaging algorithms in ultra-wideband radar systems using active aperture synthesis and stochastic probing signals. *Radioelectronic and Computer Systems*, 2023, no. 1, pp. 55-76. doi: https://doi.org/10.32620/reks.2023.1.05.
39. Maksymenko-Sheiko K.V., Sheiko T.I., Lisin D.O., Petrenko N.D. Mathematical and Computer Modeling of the Forms of Multi-Zone Fuel Elements with Plates. *Journal of Mechanical Engineering*, 2022, vol. 25, no. 4, pp. 32-38. doi: https://doi.org/10.15407/pmach2022.04.032.
40. Hontarovskyi P.P., Smetankina N.V., Ugrimov S.V., Garmash N.H., Melezhyk I.I. Computational Studies of the Thermal Stress State of Multilayer Glazing with Electric Heating. *Journal of Mechanical Engineering*, 2022, vol. 25, no. 1, pp. 14-21. doi: https://doi.org/10.15407/pmach2022.02.014.
41. Kostikov A.O., Zevin L.I., Krol H.H., Vorontsova A.L. The Optimal Correcting the Power Value of a Nuclear Power Plant Power Unit Reactor in the Event of Equipment Failures. *Journal of Mechanical Engineering*, 2022, vol. 25, no. 3, pp. 40-45. doi: https://doi.org/10.15407/pmach2022.03.040.
42. Rusanov A.V., Subotin V.H., Khoryev O.M., Bykov Y.A., Korotaiev P.O., Ahibalov Y.S. Effect of 3D Shape of Pump-Turbine Runner Blade on Flow Characteristics in Turbine Mode. *Journal of Mechanical Engineering*, 2022, vol. 25, no. 4, pp. 6-14. doi: https://doi.org/10.15407/pmach2022.04.006.
43. Sushchenko O., Averyanova Y., Ostroumov I., Kuzmenko N., Zaliskyi M., Solomentsev O., Kuznetsov B., Nikitina T., Havrylenko O., Popov A., Volosyuk V., Shmatko O., Ruzhentsev N., Zhyla S., Pavlikov V., Dergachov K., Tserne E. Algorithms for Design of Robust Stabilization Systems. *Computational Science and Its Applications – ICCSA 2022. ICCSA 2022. Lecture Notes in Computer Science*, 2022, vol. 13375, pp. 198-213. doi: https://doi.org/10.1007/978-3-031-10522-7_15.
44. Zhyla S., Volosyuk V., Pavlikov V., Ruzhentsev N., Tserne E., Popov A., Shmatko O., Havrylenko O., Kuzmenko N., Dergachov K., Averyanova Y., Sushchenko O., Zaliskyi M., Solomentsev O., Ostroumov I., Kuznetsov B., Nikitina T. Statistical synthesis of aerospace radars structure with optimal spatio-temporal signal processing, extended observation area and high spatial resolution. *Radioelectronic and Computer Systems*, 2022, no. 1, pp. 178-194. doi: https://doi.org/10.32620/reks.2022.1.14.
45. Wang D., Yu Q. Review on the development of numerical methods for magnetic field calculation of ships. *Ships Science and Technology*, 2014, vol. 36, no. 3, pp. 1-6.
46. Jin H., Wang H., Zhuang Z. A New Simple Method to Design Degaussing Coils Using Magnetic Dipoles. *Journal of Marine Science and Engineering*, 2022, vol. 10, no. 10, art. no. 1495. doi: https://doi.org/10.3390/jmse10101495.
47. Chadebec O., Rouve L.-L., Coulomb J.-L. New methods for a fast and easy computation of stray fields created by wound rods. *IEEE Transactions on Magnetics*, 2002, vol. 38, no. 2, pp. 517-520. doi: https://doi.org/10.1109/20.996136.
48. Baranov M.I., Rozov V.Y., Sokol Y.I. To the 100th anniversary of the National Academy of Sciences of Ukraine – the cradle of domestic science and technology. *Electrical Engineering & Electromechanics*, 2018, no. 5, pp. 3-11. doi: https://doi.org/10.20998/2074-272X.2018.5.01.

Received 10.04.2024
Accepted 30.06.2024
Published 02.01.2025

B.I. Kuznetsov[1], *Doctor of Technical Science, Professor,*
T.B. Nikitina[2], *Doctor of Technical Science, Professor,*
I.V. Bovdui[1], *PhD, Senior Research Scientist,*
K.V. Chunikhin[1], *PhD, Senior Research Scientist,*
V.V. Kolomiets[2], *PhD, Assistant Professor,*
B.B. Kobylianskyi[2], *PhD, Assistant Professor,*
[1] Anatolii Pidhornyi Institute of Power Machines and Systems of the National Academy of Sciences of Ukraine,
2/10, Komunalnykiv Str., Kharkiv, 61046, Ukraine,
e-mail: kuznetsov.boris.i@gmail.com (Corresponding Author)
[2] Bakhmut Education Research and Professional Pedagogical Institute V.N. Karazin Kharkiv National University,
9a, Nosakov Str., Bakhmut, Donetsk Region, 84511, Ukraine.

How to cite this article:
Kuznetsov B.I., Nikitina T.B., Bovdui I.V., Chunikhin K.V., Kolomiets V.V., Kobylianskyi B.B. Multispheroidal model of magnetic field of uncertain extended energy-saturated technical object. *Electrical Engineering & Electromechanics*, 2025, no. 1, pp. 48-55. doi: https://doi.org/10.20998/2074-272X.2025.1.07